Temperature dependence of the dielectric function and the interband critical-point parameters of GaSb

Stefan Zollner, Miquel Garriga,* Josef Humlíček,† Sudha Gopalan, and Manuel Cardona‡
Max-Planck-Institut für Festkörperforschung, Heisenbergstrasse 1, D-7000 Stuttgart 80, Germany
(Received 13 August 1990)

We have used spectroscopic ellipsometry to measure the dielectric function $\epsilon(\omega)$ of GaSb from 10 to 740 K in the 1.4–5.6 eV photon-energy region. By performing a line-shape analysis of the observed structures, the interband critical-point parameters (strength, threshold energy, broadening, and excitonic phase angle) and their temperature dependence have been determined. The observed decrease in energy after correction for the effect of thermal expansion and the corresponding increase in broadening with increasing temperature agree well with the results of a calculation that takes into account the Debye-Waller and self-energy terms of the deformation-potential-type electron-phonon interaction.

I. INTRODUCTION

GaSb with its low band gap is an important material for optoelectronic and electronic devices and is especially suited for lasers operating in the 1.2–3.0-μm-wavelength range[1–3] and for hot-electron transistors.[4] It has also been used for GaSb-AlSb quantum wells[5–10] and as a substrate for ternary[11] and quaternary[12] alloys. For a thorough understanding of these devices, a detailed knowledge of the band structure, along with the dielectric function (DF) $\epsilon(\omega)$ and their temperature dependence, is essential.

The DF of a semiconductor is closely related to its band structure, and conclusions about the bands can be drawn from features called critical points (CP's) in the $\epsilon(\omega)$ spectra, which arise from singularities in the joint density of states.[13] In the vicinity of such CP's, $\epsilon(\omega)$ can be described in terms of standard analytic line shapes:[14,15]

$$\epsilon(\omega)=C-Ae^{i\phi}(\hbar\omega-E+i\Gamma)^n . \quad (1)$$

The critical-point parameters (amplitude A, energy threshold E, broadening Γ, and excitonic phase angle ϕ) can be determined by fitting the experimental spectra $\epsilon(\omega)$ or their numerically evaluated first, second, or third derivatives to the line shapes obtained from Eq. (1). The value n is related to the dimension of the CP. C is the nonresonant contribution to the DF caused by CP's at different energies.

In the past few years, our group has been engaged in the systematic investigation of the dependence of the DF and interband CP's on temperature,[16–23] concentration of donors and acceptors,[24,25] and composition in mixed crystals,[26–28] using the technique of spectroscopic ellipsometry.[29] Parallel to this experimental work, calculations of the energy shifts and broadenings with temperature have been performed, taking into account the Debye-Waller[30,31] and self-energy terms of the deformation-potential-type electron-phonon interaction.[32–39] In this paper we investigate ellipsometrically the temperature dependence of the optical constants and CP parameters of undoped GaSb for temperatures from 20 to 750 K in the photon-energy range 1.4 to 5.6 eV and compare the CP energies and broadenings with the theoretical predictions.

The band structure of GaSb, as calculated by Chelikowsky and Cohen[40] using the empirical pseudopotential approach with spin-orbit splitting, is shown in Fig. 1. Several interband transitions related to CP's at different parts of the Brillouin zone (BZ) are indicated. Such CP's have been studied extensively using luminescence[41–45] (for the E_0 and $E_0+\Delta_0$ transitions), absorption,[46–49] magnetoabsorption,[50] resonant Raman scattering,[51,52] laser emission,[1,53] photoemission,[54,55] magnetophotoconductivity,[56] reflectance,[57–63] and several reflectance-modulation techniques, such as thermoreflectance,[64] electroreflectance,[11,65–67,45] wavelength-modulated reflectance,[68–70] and stress-modulated magnetoreflectivity.[71–73] However, relatively little work has been done regarding the temperature dependence of the CP's. The shift of the fundamental band gap has been measured up to room temperature (RT) by absorption,[46] luminescence,[45] and laser emission;[1,53] the E_1 and E_2 CP's were investigated between 100 and 500 K using absorption,[49] wavelength modulation,[68] and reflectance.[59,58]

The lowest band gap E_0 in GaSb ($\sim$820 meV at 10 K; see Ref. 67) is below the energy range of our ellipsometer. The $E_0+\Delta_0$ CP with an energy of 1.575 eV in GaSb (see Ref. 67) has not been observed in this investigation. However, this feature has been seen in GaAs,[21] GaP,[23] and InP (Ref. 22) using ellipsometry. This may be because the electron mass in GaSb is smaller[74] than in the other three materials and thus the oscillator strength for this excitonically enhanced transition is reduced. (This has been shown both theoretically[75,76] and experimentally.[77])

We present data for the E_1 and $E_1+\Delta_1$ CP's between 2 and 3 eV and for several weaker structures at higher energies. We summarize the experimental procedure in Sec. II and present the measured CP parameters and their temperature dependences in Sec. III. Finally, in

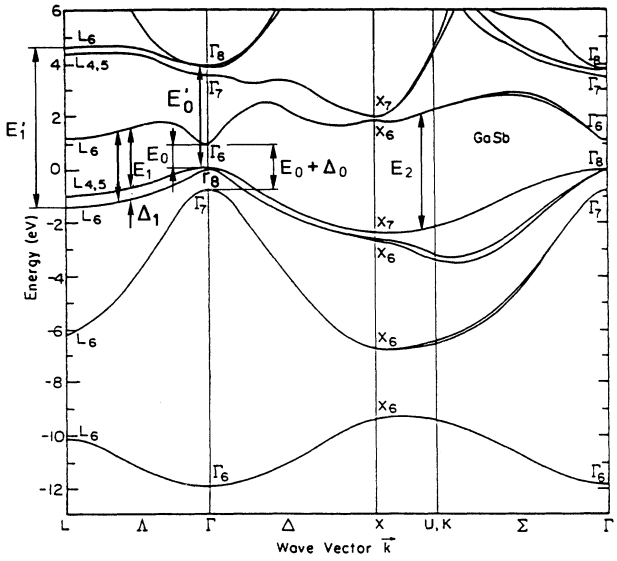

FIG. 1. Calculated band structure of GaSb, taken from Ref. 40. Several interband critical-point (CP) transitions are indicated. The assignment of the E_2 critical point is tentative.

Sec. IV, we calculate the CP shifts and broadenings, taking into account the thermal expansion term and the Debye-Waller and self-energy terms of the deformation-potential-type electron-phonon interaction[38] and compare them with those obtained experimentally.

II. EXPERIMENT

The measurements were performed on samples cut from a nominally undoped (p-type) ingot with (111) surface orientation. Undoped grown GaSb crystals are always p type because of native lattice defects. The defect is a combination of a Ga vacancy and a Ga atom on a Sb site which acts as a doubly ionizable acceptor.[45] Before mounting the sample into the cryostat, a wet-chemical etching process[29,78] was performed in order to remove the oxide layer on the surface.[21] Figure 2 shows the pseudo-dielectric function thus obtained at room temperature and corrected for a 0.5-nm oxide layer[79] (solid line) in comparison with the data of Ref. 29 (symbols). The correction was necessary to achieve agreement of both spectra at the peak of ϵ_2 at 4.04 eV. After etching, the sample was quickly mounted inside a cryostat and measured at several temperatures between 10 and 740 K. Figure 2 also shows a spectrum of a sample measured at RT in the cryostat and corrected for an oxide film of 1.8 nm on the surface (dotted line). Again, the correction was made in order to achieve agreement with the data of Ref. 29. The measurements were taken with an automatic spectral ellipsometer of rotating analyzer type.[80] The angle of incidence was always kept at 67.5° and the polarizer angle at 30°.

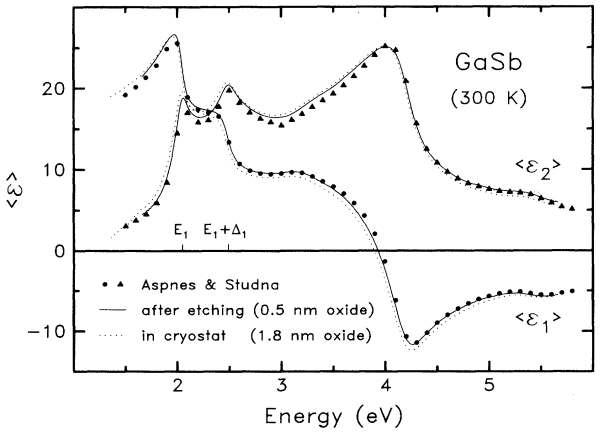

FIG. 2. Real (ϵ_1) and imaginary (ϵ_2) part of the dielectric function vs energy, obtained directly after etching (solid line, corrected for 0.5-nm oxide) and after mounting inside the cryostat (dotted line, corrected for 1.8-nm oxide) in comparison with data from Ref. 29 (●, ▲).

III. RESULTS AND DISCUSSION

In Figs. 3 and 4 we present the spectra obtained for the real and imaginary parts of the dielectric function of GaSb for several temperatures after applying a correction for 1.8 nm of oxide on the GaSb surface. Three structures, corresponding to the E_1, $E_1+\Delta_1$, and E_2 transitions, are clearly resolved. At low temperatures, several little bumps between 3 and 3.5 eV and a broad peak at 5.11 eV can be seen. The origin of these features will be discussed later. In order to perform a line-shape analysis [see Eq. (1)] and obtain the critical-point parameters, we calculated numerically[81] the third derivative of the observed spectra (see Fig. 5). The resulting curves are qualitatively similar to those observed in electroreflectance.[67] Both the real and the imaginary parts of $d^3\epsilon/dE^3$ were fitted simultaneously, using a least-squares procedure. A recent numerical study[82] has shown that this procedure gives more accurate CP parameters than any other modulation technique. The arrows in Fig. 5 indicate the CP energies thus obtained. These energies are presented

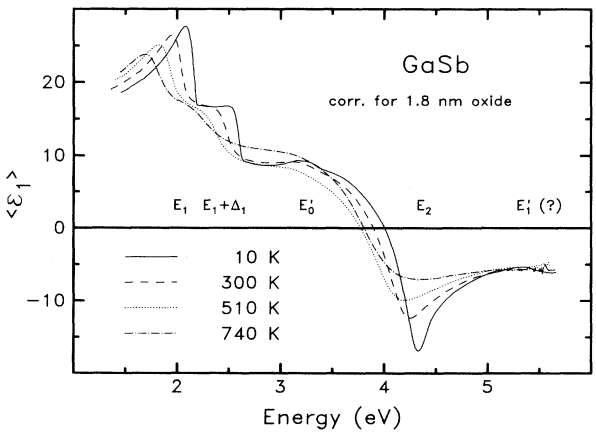

FIG. 3. Real part of the dielectric function (ϵ_1) at different temperatures, corrected for an oxide layer of 1.8 nm.

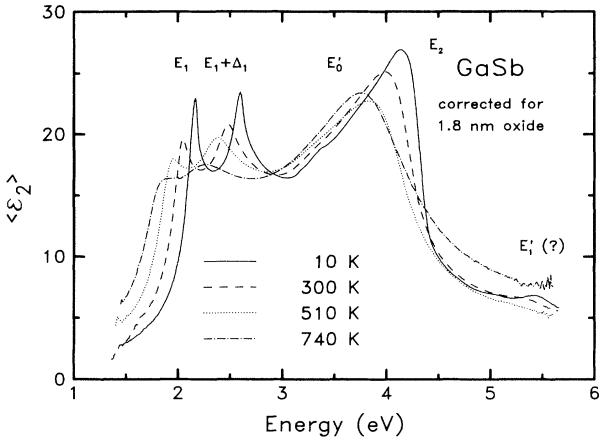

FIG. 4. As Fig. 3, but for ϵ_2.

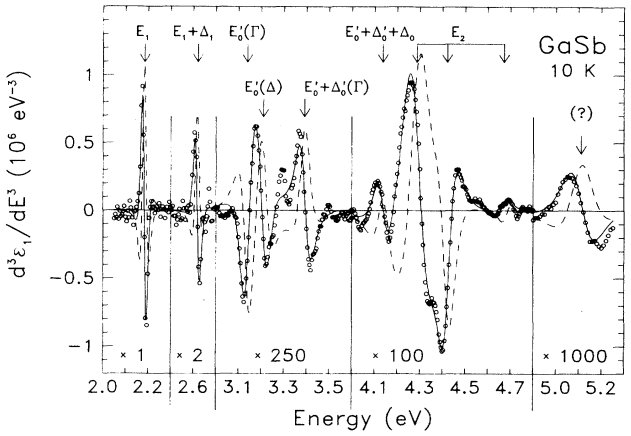

FIG. 5. Numerically calculated third derivative of ϵ_1 at 10 K in the vicinity of CP's (○), together with a line-shape fit according to Eq. (1) (solid line). The dashed line gives the imaginary part of the fit. The readings on the vertical sale have to be divided by the factors given below the structures. The arrows indicate the energy positions of the CP's.

in Table I along with the line shapes used and the parameters [see Eq. (1)] obtained from the fit.

Since the features in the spectra become sharper and more distinct at low temperatures, we use the spectra measured at 10 K to discuss the origin and character of the various interband CP's observed. At 2.184 and 2.618 eV we find two very strong features labeled E_1 and $E_1+\Delta_1$. They are known to be produced by transitions from the $\Lambda_{4,5}$ and Λ_6 valence bands (VBs), respectively, to the Λ_6 conduction band (CB) extending to the L point of the BZ.[67,83] These structures are very strong and are observed up to 790 K. At temperatures below 600 K they could be fitted slightly better with a Lorentzian (excitonic) line shape than with a 2D CP. The phase angle ϕ of these two CP's was forced to be the same fitted value (about 90° at RT for a 2D line shape). A constant spin-orbit splitting $\Delta_1=442$ meV, obtained from measurements at room temperature, was assumed for temperatures above 500 K. Over the temperature range below 500 K the energy difference Δ_1 between the two CP's stayed approximately constant at 441(6) meV, with an increase from 434(1) meV at 10 K to 442(1) meV at 300 K and 447 meV at 500 K. This slight increase (13 meV) could be due to numerical errors caused by the fitting procedure.[82]

Between 3.1 and 4.2 eV we find four very weak structures which could only be resolved between 10 and 86 K. The parameters of the line-shape fit at 10 K are given in Table I. The origin of this quadruplet is somewhat controversial.[67] In analogy with germanium, the triplet $E_0'=3.139$ eV, $E_0'+\Delta_0'=3.391$ eV, and $E_0'+\Delta_0'+\Delta_0=4.135$ eV is usually assigned to transitions at or near Γ from the highest VB (Γ_7^v,Γ_8^v) to the second lowest CB (Γ_7^c,Γ_8^c) along with their spin-orbit split states (and therefore fitted with 3D line shapes). Δ_0 and Δ_0' are the corresponding spin-orbit splittings of the Γ_{15} valence and conduction bands. The $E_0'+\Delta_0$ structure ($\Gamma_7^v\rightarrow\Gamma_7^c$) is suppressed by symmetry (exactly forbidden at Γ; see Ref. 84). The spin-orbit splitting of the valence band $\Delta_0=4.135$ eV -3.391 eV$=744$ meV thus obtained is in excellent agreement with $\Delta_0=753$ meV measured directly from transitions to the lowest CB edge.[67] Furthermore, the peaks at 4.135 and 3.391 eV have the same phase angle $\phi\simeq 110°$. This suggests that they are related CP's. The phase angle of the E_0' CP was found to be about 270°

TABLE I. Fit parameters of the CP's between 2 and 5 eV at 10 K. For a 3D (0D) CP the amplitudes A have the dimension $\text{eV}^{-0.5}$ (eV); they are dimensionless for a 2D CP. The numbers in parentheses give the errors (95% confidence limits).

GaSb	E (eV)	Γ (meV)	ϕ (deg)	A	Line shape
E_1	2.184(1)	195(5)	180(4)	4.6(4)	2D
E_1	2.184(1)	269(6)	90(5)	0.10(1)	0D
$E_1+\Delta_1$	2.618(1)	230(20)	180(4)	2.4(5)	2D
$E_1+\Delta_1$	2.618(1)	320(20)	90(5)	0.06(2)	0D
$E_0'(\Gamma)$	3.139(1)	49(3)	270(fixed)	4.6(8)	3D
$E_0'(\Delta)$	3.211(4)	58(5)	223(9)	0.24(6)	2D
$E_0'(\Gamma)+\Delta_0'$	3.391(3)	51(3)	125(7)	3.8(5)	3D
$E_0'(\Gamma)+\Delta_0'+\Delta_0$	4.135(5)	53(5)	116(13)	5(1)	3D
$E_2(1)$	4.286(3)	108(3)	150(4)	7.1(5)	2D
$E_2(2)$	4.419(3)	71(3)	319(7)	1.3(1)	2D
$E_2(3)$	4.68(1)	54(13)	64(39)	0.07(5)	2D
Δ(?)	5.11(1)	130(10)	174(12)	10(2)	2D

TABLE II. Experimental and theoretical critical-point (CP) energies (in eV) for GaSb at several temperatures T (in K). There is some scatter in the experimental data, probably due to inadequate sample quality or surface preparation, or an inadequate line-shape analysis.

T	E_0	$E_0+\Delta_0$	E_1	$E_1+\Delta_1$	E_0' region	E_2 region	E_1' region
				Experiment			
4	0.798 (Ref. 46)						
	0.813 (Ref. 50)	1.575 (Ref. 43)					
	0.8112 (Ref. 56)		2.154 (Ref. 68)	2.596 (Ref. 68)	3.35,3.69 (Ref. 68)	4.35,4.55,4.75,5.07 (Ref. 68)	5.51,5.65 (Ref. 68)
10	0.822 (Ref. 67)	1.575 (Ref. 67)	2.195 (Ref. 67)	2.625 (Ref. 67)	3.191,3.404,4.160 (Ref. 67)	4.36,4.40,4.72 (Ref. 67)	5.37,5.46,5.59 (Ref. 67)
	0.810 (Ref. 48)		2.184[a]	2.619[a]	3.138,3.210,3.391,4.135[a]	4.286,4.419,4.68[a]	5.11[a]
20	0.810 (Ref. 41)		2.195 (Ref. 73)				
27	0.808 (Ref. 11)	1.569 (Ref. 11)	2.185 (Ref. 11)	2.622 (Ref. 11)			
30	0.811 (Ref. 71)	1.561 (Ref. 71)					
77	0.784 (Ref. 46)		2.20 (Ref. 51)	2.65 (Ref. 51)			
			2.08 (Ref. 60)	2.55 (Ref. 60)	3.74 (Ref. 60)	4.33,4.70 (Ref. 60)	
			2.155 (Ref. 69)	2.597 (Ref. 69)			
			2.13 (Ref. 64)	2.60 (Ref. 64)	3.2,3.6,3.8 (Ref. 64)	4.40,4.75 (Ref. 64)	
	0.80 (Ref. 47)		2.095 (Ref. 70)	2.533 (Ref. 70)	3.31,3.70,3.85 (Ref. 70)	4.10,4.22,4.68 (Ref. 70)	
					3.160,3.375,4.110 (Ref. 66)		
86			2.169[a]	2.605[a]	3.13,3.21,3.39,4.11[a]	4.268,4.397,4.67[a]	
295	0.704 (Ref. 46)		2.07 (Ref. 49)	2.56 (Ref. 49)		4.28,4.55,4.62 (Ref. 62)	5.60,5.73 (Ref. 62)
			2.015 (Ref. 58)	2.46 (Ref. 58)		4.25 (Ref. 58)	
	0.70 (Ref. 59)		2.02 (Ref. 59)	2.48 (Ref. 59)		4.3 (Ref. 59)	
300	0.725 (Ref. 11)	1.485 (Ref. 11)	2.055 (Ref. 11)	2.490 (Ref. 11)	3.7,4.4 (Ref. 54)	4.17,4.5 (Ref. 54)	5.7 (Ref. 54)
	0.725 (Ref. 47)	1.524 (Ref. 45)	2.09 (Ref. 52)				
			2.00 (Ref. 57)	2.48 (Ref. 57)		4.22 (Ref. 57)	
		1.52 (Ref. 65)	2.03 (Ref. 65)	2.49 (Ref. 65)	3.27,3.56,3.85 (Ref. 65)	4.2,4.57 (Ref. 65)	5.5 (Ref. 65)
			2.052[a]	2.494[a]		4.20[a]	
500			1.923[a]	2.370[a]		4.08[a]	
4	$\Delta_0=0.752$ (Ref. 43)						
30	$\Delta_0=0.749$ (Ref. 72)						
300	$\Delta_0=0.82$ (Ref. 55)		$\Delta_1=0.45$ (Ref. 55)			$\Delta_2=0.24$ (Ref. 55)	
				Theory			
0	0.86 (Ref. 87)	1.62 (Ref. 87)	2.22 (Ref. 87)	2.67 (Ref. 87)	3.44,3.77,4.53 (Ref. 87)	4.84,5.12 (Ref. 87)	5.43,5.59 (Ref. 87)
						4.09,4.16,4.33,4.40 (Ref. 87)	
	1.00 (Ref. 93)		2.41 (Ref. 93)		3.43 (Ref. 93)	3.84,4.14 (Ref. 93)	5.27 (Ref. 93)
	$\Delta_0=0.67$ (Ref. 88)		$\Delta_1=0.40$ (Ref. 88)		$\Delta_0'=0.27$ (Ref. 88)	$\Delta_2=0.25$ (Ref. 88)	$\Delta_1'=0.15$ (Ref. 88)
	$\Delta_0=0.727$ (Ref. 90)		$\Delta_1=0.415$ (Ref. 90)			$\Delta_2=0.256$ (Ref. 90)	
	$\Delta_0=0.64$ (Ref. 89)		$\Delta_1=0.37$ (Ref. 89)		$\Delta_0'=0.26$ (Ref. 89)	$\Delta_2=0.37$ (Ref. 89)	$\Delta_1'=0.13$ (Ref. 89)
	$\Delta_0=0.81$ (Ref. 91)		$\Delta_1=0.39$ (Ref. 65)		$\Delta_0'=0.31$ (Ref. 65)	$\Delta_2=0.29$ (Ref. 65)	$\Delta_1'=0.16$ (Ref. 65)
	$\Delta_0=0.73$ (Ref. 92)					$\delta=-0.34$ (Ref. 86)	
	$\Delta_0=0.67$ (Ref. 94)				$\Delta_1=0.22$ (Ref. 94)		

[a]Present work.

when fitted with a 3D line shape. The fourth peak (at 3.211 eV) was not observed by Aspnes *et al.* in GaSb,[67] but an equivalent one was seen in a similar study on GaAs;[85] it is tentatively assigned to transitions near the pseudocrossing (or crossing; see Ref. 86) of the two lowest CB's along the Δ direction near Γ (see Ref. 85). It was fitted with a 2D line shape. The additional structure at 3.3 eV (see Fig. 5) is probably due to excitonic effects and should not be attempted to fit.

Above 4 eV we find the familiar[67] E_2 triplet [$E_2(1)=4.286$, $E_2(2)=4.419$, and $E_2(3)=4.68$ eV], probably[67,40] due to transitions at X, along Δ, or from a plateau near the point $P=(2\pi/a)(\frac{3}{4},\frac{1}{4},\frac{1}{4})$, where a is the lattice constant. These structures were fitted with 2D line shapes. As $E_2(1)$ and $E_2(2)$ overlap with each other and with $E_0'+\Delta_0'+\Delta_0$ and the broadenings of the structures are comparable with their energy separation, all three structures had to be fitted simultaneously. The fit only gave reasonable results below 80 K (see Table I). At higher temperatures (up to 750 K) the three CP's were fitted as one structure. The strongest of these three structures (see the amplitudes in Table I) is probably due to transitions near P and therefore labeled $E_2(1)=E_2(P)=4.286$ eV. Another transition with medium strength is expected from band-structure calculations[40] along Δ near 4.37 eV. We therefore assign $E_2(2)=E_2(\Delta)=4.419$ eV. The third structure is very weak and could be due to transitions at X from the doublet in the valence band (separated by the spin-orbit splitting $\Delta_2=0.24$ eV; see Refs. 55 and 40) to the corresponding doublet in the conduction band (split by the heteropolar gap $\delta\sim 0.33$ eV). We therefore assign $E_2(3)=E_2(X_6^v\rightarrow X_7^c)=4.68$ eV. This is compatible with the structure $E_2(X_7^v\rightarrow X_6^c)$ at 4.16 eV seen by Aspnes,[67] but not by us. The three remaining transitions of this quadruplet at X (which are not suppressed by symmetry) are probably hidden by the other strong transitions in this energy range.

Finally, we observe a very weak structure at 5.11(1) eV that is too low in energy to be assigned to the E_1' (5.5 eV; see Ref. 67), transitions from the $\Lambda_{4,5}$ VB to the $\Lambda_{4,5}$ CB. It was also observed by Aspnes[67] and assigned to transitions along Δ from the highest VB to the lowest CB in Ref. 40.

In Table II we give an overview of our experimentally obtained CP energies at 10, 86, 300, and 500 K, in comparison with other experimental values from the literature. The theoretical values of the corresponding CP energies at $T=0$ obtained from different band-structure calculations[86–94] are also presented. It can be seen that our data agree very well with the accurate electroreflectance data of Ref. 67, whereas other data show more dispersion, probably due to poor sample quality or preparation or inadequate analysis of the data. We have performed a complete line-shape analysis in order to accurately determine the CP parameters.[82]

The energies for the E_1, $E_1+\Delta_1$, and E_2 CP's as a function of temperature are shown in Fig. 6, with $E_0'+\Delta_0'+\Delta_0$, $E_2(1)$, and $E_2(2)$ fitted as one structure E_2 (because of poor resolution at high temperatures). The dotted curves obtained from the theoretical calculations are discussed in Sec. IV. The solid lines represent a fit of

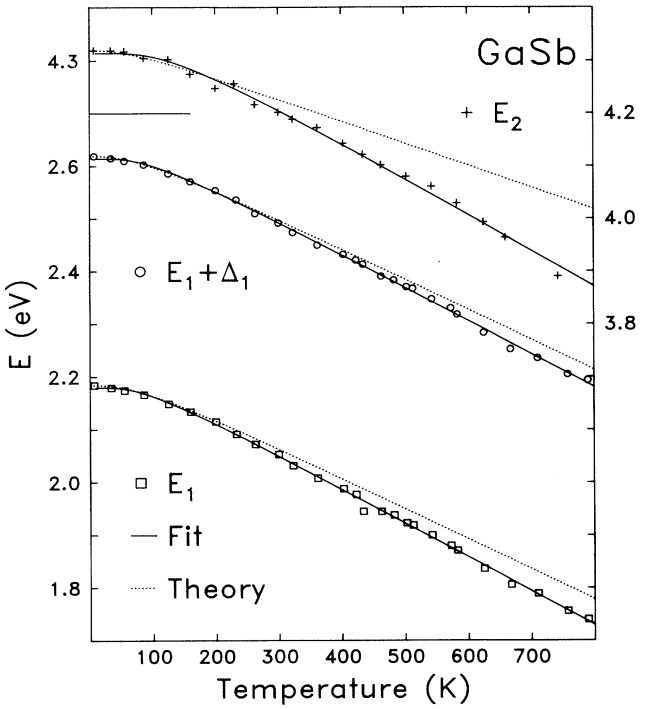

FIG. 6. Temperature dependences of the interband critical-point energies of GaSb as obtained from a line-shape fit to ellipsometric data. The solid lines represent the best fits with Eq. (2); the dotted ones give the result of a parameter-free calculation as outlined in the text.

the data with a semiempirical model[21] of the temperature change of the band structure due to the electron-phonon interaction:[38]

$$E(T)=E_B-2a_B\left[\frac{1}{2}+\frac{1}{e^{\Theta/T}-1}\right]. \tag{2}$$

The parameter Θ describes a mean frequency of the phonons involved and a_B is the strength of the virtual transition causing the energy shifts. E_B is related to the energy of the CP. We have also performed a fit with the semiempirical Varshni law[95]

$$E(T)=E(0)-\frac{\alpha T^2}{T+\beta}, \tag{3}$$

where $E(0)$ is the energy of the CP extrapolated to zero temperature and α and β are empirical parameters. The results of the fits with both models are given in Table III. We also give linear temperature coefficients of the CP energies in Table IV. We compare them with those obtained experimentally by other authors, in most cases averaged between 100 and 300 K. The theoretical values obtained from a microscopic calculation of the deformation-potential-type electron-phonon interaction are also presented in the table and will be discussed in detail in Sec. IV. Manoogian and Wooley[96] have shown that β in Eq. (3) should be equal to one-half the Einstein temperature, if the thermal expansion contribution to the shifts (see Sec. IV) is small, which implies $\beta=150$ K for GaSb. From Table III it can be seen that this interpretation holds well, except for the E_2 gap.

TABLE III. Parameters E_B, Θ, and a_B obtained by fitting the CP energies versus temperature to Eq. (2), and values of $E(0)$, α, and β obtained by fitting with Eq. (3). The numbers in parentheses indicate the 95% error margins. Values for E_0 were taken from the literature.

	E_B (eV)	a_B (meV)	Θ (K)	$E(0)$ (eV)	α (10^{-4} eV K^{-1})	β (K)	Line shape
E_1	2.254(12)	74(16)	227(43)	2.186(7)	6.8(3)	147(46)	Excitonic
$E_1+\Delta_1$	2.695(11)	81(14)	254(39)	2.621(5)	6.7(3)	176(41)	Excitonic
E_2	4.44(3)	124(37)	356(86)	4.320(8)	9(1)	376(146)	2D
E_0				0.812	4.2	140	From Ref. 45
E_0				0.810	3.8	94	From Ref. 31

The temperature dependences of the broadenings of the E_1, $E_1+\Delta_1$, and E_2 CP's obtained from the experimental spectra are given in Fig. 7. The theoretical curves (dotted and dashed lines) will be discussed in Sec. IV. Fits to the broadenings as a function of temperature (solid lines in Fig. 7) are performed with the equation

$$\Gamma(T)=2\Gamma_0\left[\frac{1}{2}+\frac{1}{e^{\Theta/T}-1}\right]+\Gamma_1\ , \tag{4}$$

where the first term describes the lifetime broadenings due to electron-phonon interaction in a similar fashion as in Eq. (2), whereas the second term accounts for other sources of broadenings, e.g., experimental resolution, sample inhomogeneity, defects, or overlap of several CP's. The resulting parameters are given in Table V with their 95% confidence limits. In the fit to the broadenings of the $E_1+\Delta_1$ CP, the last four data points above 650 K were omitted as their error bars are very large. The values for Θ in Eqs. (2) and (4) for shifts and broadenings need not be the same, since only energy-conserving self-energy processes contribute to the latter while virtual transitions plus Debye-Waller terms determine the former (see Sec. IV). Fortuitously, they are nearly the same for the fits to the shifts and broadenings. The parameter Γ_1 is small for E_1 and $E_1+\Delta_1$, but large for E_2 since the three overlapping CP's $E_0'+\Delta_0'+\Delta_0$, $E_2(1)$, and $E_2(2)$ were fitted as one structure.

The remaining two parameters used in fitting the CP line shapes according to Eq. (1) are the phase angle ϕ, which describes the type of CP together with excitonic effects, and the amplitude A. These are plotted as func-

TABLE IV. Linear temperature coefficients of CP energies for GaSb (in 10^{-4} eV/K).

$\frac{dE_0}{dT}$	$\frac{dE_1}{dT}$	$\frac{dE_2}{dT}$
	Experiment	
	Between 100 and 300 K	
4.1[a]	4.0[b]	4.1[c]
2.9[d]	4.2[e]	
2.8[f]	4.5[c]	
3.7[g]	5.7[h]	5.5[h]
	Between 300 and 500 K	
	4.6[i]	6.2[i]
	6.4[h]	6.1[h]
	Theory (at 300 K)	
4.7[j]	5.2[j]	3.7[j]
1.4[k]	0.8[k]	0.6[k]
2.4[l]		
4.3[m]	4.0[m]	4.0[m]

[a]Reference 46.
[b]Reference 49.
[c]Reference 68.
[d]Reference 47.
[e]Reference 59.
[f]Reference 53.
[g]Reference 31.
[h]Present work.
[i]Reference 58.
[j]Thermal expansion, self-energy, and Debye-Waller terms (present work).
[k]Thermal expansion only (present work).
[l]Debye-Waller term only, from Ref. 31.
[m]Debye-Waller term only (present work).

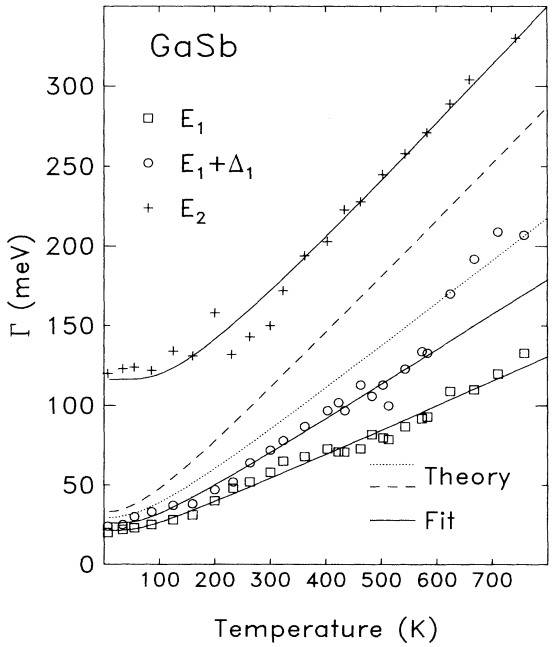

FIG. 7. Temperature dependences of the CP broadenings of GaSb. The solid lines show the result of a least-squares fit to Eq. (4); the dotted (E_1) and dashed (E_2) ones were obtained from the theory of the electron-phonon interaction. A broadening of 60 meV at 77 K was found for the E_1 gap in Ref. 51.

TABLE V. Parameters used to fit the temperature dependence of the broadenings in GaSb, as described in Eq. (4). The numbers in parentheses indicate the 95% error margins.

	Γ_1 (meV)	Γ_0 (meV)	Θ (K)	Line shape
E_1	6(8)	15(12)	200(140)	2D
E_1	10(11)	20(16)	180(140)	Excitonic
$E_1+\Delta_1$	2(14)	24(19)	220(140)	2D
$E_1+\Delta_1$	5(14)	30(19)	200(110)	Excitonic
E_2	46(10)	70(5)	377(fixed)	2D

tions of temperature in Figs. 8 and 9. The phase angle of E_1, when fitted with a 2D line shape, seems to approach 0° at high temperatures, as expected for a 2D minimum. The angle is larger than this value due to excitonic effects. The phase angle of $E_1+\Delta_1$ was set equal to that of E_1 during the fitting procedure. The dimensionless amplitudes for the E_1 and $E_1+\Delta_1$ transitions fitted with a 2D line shape can be estimated within $\mathbf{k}\cdot\mathbf{p}$ theory:[14,21]

$$A_{E_1}\cong\frac{44(E_1+\Delta_1/3)}{aE_1^2}=3.8\ ,$$
$$A_{E_1+\Delta_1}\cong\frac{44(E_1+2\Delta_1/3)}{a(E_1+\Delta_1)^2}=2.7\ , \tag{5}$$

where the lattice constant a is in Å and the energies E_1 and Δ_1, taken at 300 K, are in eV. The agreement with the experiment ($A_{E_1}=6\pm1$, $A_{E_1+\Delta_1}=3.0\pm0.5$) is reasonable and can be improved by taking into account corrections for terms linear in $\mathbf{k}$ for $\mathbf{k}$ perpendicular to the $\langle 111\rangle$ direction,[63] which increases A_{E_1} and decreases

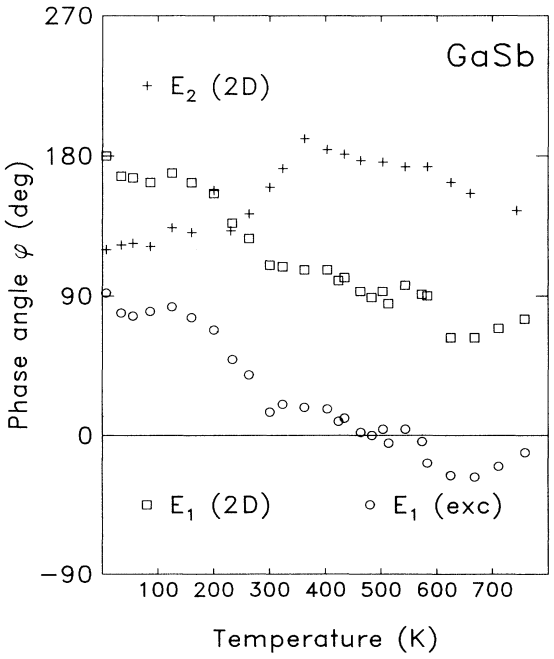

FIG. 8. Temperature dependences of the CP phase angles of GaSb.

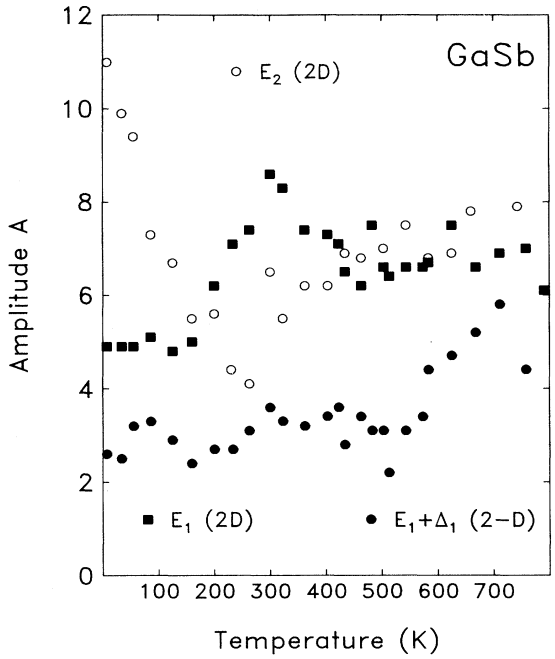

FIG. 9. Temperature dependences of the CP amplitudes of GaSb.

$A_{E_1+\Delta_1}$. Furthermore, the excitonic interaction should increase the theoretical estimates. The evaluation of the excitonic (0D) amplitudes is more difficult, as details about screening of the excitonic (Coulomb) interaction have to be known. Equation (19) of Ref. 21 gives $A_{E_1}=0.015$ eV and $A_{E_1+\Delta_1}=0.012$ eV for the Lorentzian (0D) amplitudes when the static dielectric constant $\epsilon_s=15.7$ is used. These theoretical estimates are about one order of magnitude smaller than the fitted 0D amplitudes $A_{E_1}=0.1(0.7)$ eV and $A_{E_1+\Delta_1}=0.07(0.4)$ eV at 10 (700) K. This discrepancy has also been found in GaAs (Ref. 21) and was attributed to the fact that the excitonic Bohr radius might be smaller than or comparable to the screening length of the Coulomb potential, a fact which may require the use of a smaller value of ϵ.

IV. THEORY

In this section we discuss our theoretical results for the shifts and broadenings of the CP's with temperature. The shifts of the critical-point (CP) energies with temperature are caused by the thermal expansion (TE) of the lattice and the renormalization of the band energies by electron-phonon coupling.[38] The TE term given by

$$\left[\frac{\partial E_{\rm CP}}{\partial T}\right]_{\rm TE}=-3\alpha B\left[\frac{\partial E_{\rm CP}}{\partial p}\right]_T \tag{6}$$

can be easily calculated if the bulk modulus B, the linear TE coefficient α, and the pressure dependence of the CP energy at constant temperature are known.[97–99] For example, we obtain using the values from Table VI in Eq. (6) a linear temperature coefficient of only -0.8×10^{-4} eV/K for the E_1 CP at RT. This is less than 20% of the

TABLE VI. Data used in the calculations of the thermal expansion shifts of the CP energies.

Parameter	Unit	Value	Reference
B	GPa	56	97
$(\partial E_0/\partial p)_T$	meV/GPa	146	74
$(\partial E_1/\partial p)_T$	meV/GPa	75	97,99
$(\partial E_2/\partial p)_T$	meV/GPa	60	97,99
α (300 K)	10^{-6} K^{-1}	6	98

observed linear temperature coefficient (see Table IV). The corresponding shifts of the CP's due to the effect of thermal expansion of the lattice are evaluated by integrating Eq. (6) using the temperature-dependent linear expansion coefficients of Ref. 98. The result for the shift of the E_1 gap (due to TE) is shown by the dotted line in Fig. 10. The shift arising from this thermal expansion term is found to be negative, i.e., it leads to a band-gap narrowing.

The electron-phonon interaction, which accounts for the major portion of the energy shifts, can be treated within perturbation theory in a rigid-ion approximation taking into account the two terms quadratic in the ionic displacement,[100,38] i.e., the Fan[32] or self-energy term (arising from the first-order electron-phonon interaction taken to second order in perturbation theory) and the Debye-Waller term[30,31] (arising from the second-order electron-phonon interaction taken to first order in perturbation theory). The Feynman diagrams for both terms are given in Fig. 1 of Ref. 38. Each of the two terms has to be calculated for both the valence and conduction band at the **k** point of interest and an integration with respect to the phonon wave vector **q** over the entire Brillouin zone has to be performed.

We have calculated the temperature shifts of the CP's by including the TE term (described earlier) and both electron-phonon terms in analogy to the work on GaAs described in detail in Ref. 38. We have based the calculations of the electronic states on a local empirical pseudopotential band structure[103] without spin-orbit splitting and used a basis of 59 or 89 plane waves. An empirical 10-parameter shell model was used for the description of the phonon eigenvalues and eigenstates.[104,105] The information about the electron-phonon terms is contained in the temperature-independent, dimensionless electron-phonon spectral functions $g^2F(\Omega)$ of the self-energy and Debye-Waller terms of the valence and conduction bands, shown for example at the L point in GaSb in Fig. 11. Ω is the energy of the absorbed and emitted phonon. All spectra show four more or less distinct peaks corresponding to the zone-edge transverse acoustic (TA, centered around 6 meV), longitudinal acoustic (LA, around 18 meV), transverse optic (TO, 27 meV), and longitudinal optic (LO, 26 meV) phonons near the L point. The TO peak is missing in the self-energy spectral function of the conduction band, in analogy to calculations of the **k** dependence of intervalley deformation potentials for GaAs,[106] where it has been shown that this phonon con-

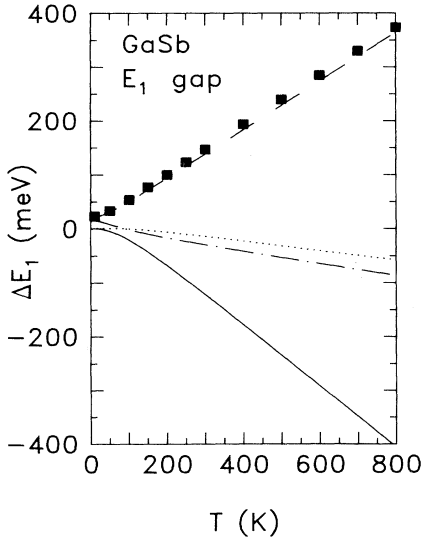

FIG. 10. The total calculated shift, i.e., self-energy, Debye-Waller, and thermal expansion term (solid line) of the E_1 gap with temperature compared with that arising from thermal expansion only (dotted line). A comparison of the total shift with the experiment is shown in Fig. 6. The *absolute shifts* of the valence band at the L point are also shown for the self-energy term (dashed-dotted line) and the Debye-Waller term (dashed line). The corresponding shift of the conduction band (not shown in the figure) is very small for the Debye-Waller term and approximately equal to that of the valence band for the self-energy term. The symbols (■) show the Debye-Waller term calculated from the Debye-Waller factors of Ref. 101 and 102.

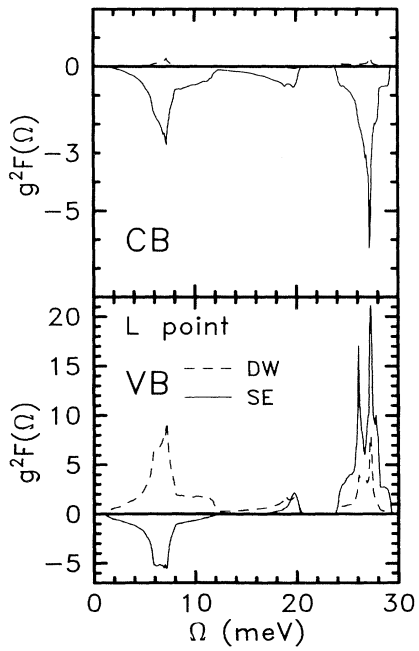

FIG. 11. Temperature-independent, dimensionless electron-phonon spectral functions for the conduction band (top) and the valence band (bottom) of GaSb at the L point. The dashed lines show the Debye-Waller terms (DW), the solid lines the self-energy terms (SE).

tributes only weakly to intervalley scattering processes between the L and Γ valleys. The corresponding shifts $\Delta E_{\mathbf{k}n}$ of the electronic states, at a given $\mathbf{k}$ point and band index n, as a function of temperature T can be obtained by integrating the spectral functions $g^2F(\Omega)$ along with the temperature-dependent phonon occupation factor $N_{\mathbf{Q}j}$ over all phonon energies Ω:

$$\Delta E_{\mathbf{k}n}(T)=\int_0^\infty g^2F(\Omega)[N_{\mathbf{Q}j}(T)+\tfrac{1}{2}]d\Omega \ . \tag{7}$$

The self-energy spectral function for the *absolute* shift of the CB at the L point (see Fig. 11) is negative, and this implies that the conduction band shifts down with increasing temperatures. The Debye-Waller (DW) spectral function for the CB is very small and positive.

The two spectral functions (shown in Fig. 11) for the valence band at the L point are much larger than their counterparts for the conduction band, because the density of states with similar energies is much larger for the L_v state than for the L_c state as the hole masses in the Γ valley are larger than the electron mass. The Debye-Waller spectral function for the valence band at L is positive, implying a shift to higher energies with increasing temperature. The self-energy spectral function is negative for the TA phonons and positive for the phonons with higher energy. Therefore, at very low temperatures, when no phonons are activated, the spectral function simply has to be integrated [as $N_{\mathbf{Q}j}=0$ at $T=0$; see Eq. (7)] and tends to shift the valence band up, whereas at elevated temperatures, when acoustic phonons have a higher occupation than optical phonons, the valence band shifts to lower energies. The largest absolute shift occurring at the L point in GaSb is due to the DW term of the valence band. It can be seen from Fig. 10 that the energy shifts of the valence band at the L point arising from the self-energy term (dashed-dotted line) is opposite in sign to that from the DW term (dashed line) and therefore the two terms tend to cancel each other. In some cases the self-energy contribution is even comparable in magnitude to the DW contribution.

An attempt to explain the negative sign of the self-energy spectral function of the conduction band (see Fig. 11) has to start with Eq. (7) of Ref. 38. We see that the sign is determined by the energy difference in the denominator. We only consider intermediate states in the conduction band since terms arising from all other intermediate states (VB) are small because of the large energy denominator. We see that the self-energy term is negative, because the density of intermediate states in the Γ valley rises steeply for energies above L_6^c. An analogous argument for the valence band shows that the self-energy spectral function should be positive, which is indeed the case for the LA phonon and the optical phonons, but fails to explain the negative contribution of the TA phonon.

The Debye-Waller terms can also be easily evaluated by including temperature-dependent Debye-Waller factors $\exp(-G^2\langle u^2\rangle/6)$ into the structure factors in the empirical pseudopotential band-structure calculation. Here G is the magnitude of the reciprocal lattice vector of the corresponding structure factor and $\langle u^2\rangle$ is the mean-squared phonon amplitude of the atom under consideration. The difference between this result (shown by the symbols ■ in Fig. 10) with that described above (dashed line in Fig. 10) is only about 6%. Half of this difference is due to an inconsistency in the Debye-Waller factors, as the two calculations are based on two different phonon models. We have checked that, when using the same phonon model for both calculations, the error introduced by integrating over the Brillouin zone is only about 3% for the valence band. We have calculated all of our Debye-Waller terms using the perturbative approach, as this does not rely on published Debye-Waller factors[101,102] and makes sure that the self-energy and Debye-Waller terms are calculated in a consistent way.

In order to now compare these results with the experimentally observed shifts of the E_1 CP, we note that the E_1 CP corresponds to transitions from the Λ_3 valence band to the Λ_6 conduction band. Hence we perform the calculations for several points in $\mathbf{k}$ space along the Λ direction and then take their average as that contributing to the E_1 CP. The result of this procedure is shown by the lowest dotted line in Fig. 6. It compares well with the experimental data, especially when considering that our theory contains no adjustable parameters. We have found that the calculated total shifts do not change much along Λ, although the individual contributions (Debye-Waller and self-energy terms) do. We have shifted the results of our nonrelativistic calculation by a constant spin-orbit splitting of $\Delta_1=441$ meV to obtain the temperature dependence of the $E_1+\Delta_1$ critical point, shown by a dotted line in Fig. 6. There is a general trend for the calculated shifts to be too small,[38,39] probably because of the error caused by integrating the self-energy with a relatively crude mesh of only 89 points in the irreducible wedge of the Brillouin zone.

We have chosen the 10-parameter shell model[104] for our calculation, because it has been shown to give the best phonon polarization vectors in GaAs.[107] We have also calculated the electron-phonon spectral functions at the L point with a 14-parameter shell model (model A of Ref. 108 with the correction given in Ref. 101). There are some differences in the phonon density of states between the two models, but the structure in the spectral function plots remains nearly the same. The energy shifts calculated with the two models disagree by only 2%.

We now proceed to discuss the temperature shifts of the E_2 CP. A detailed study of the optical properties of semiconductors using the linear muffin-tin orbitals (LMTO) approach in its scalar-relativistic form[83] indicates that the E_2 CP arises mainly from transitions from the highest valence band to the lowest conduction band in a region in the Brillouin zone around the point $\pi/2a(3,1,1)$. We therefore compare the experimental shifts of the E_2 CP with the shifts calculated for this point (see Fig. 6). It can be seen that the agreement is not too good, for the several possible reasons: (i) The E_2 critical point consists of at least three different structures that were fitted as one CP to obtain the temperature dependence of E_2 (see Table I). (ii) The location of these three structures is not well known and the single point $\pi/2a(3,1,1)$ may not represent the CP well. (iii) The error in the calculation to obtain the self-energy spectral

function may be larger for the E_2 CP than for the E_1 CP because of unknown details in the band structure.

We have also calculated the temperature shifts of the E_0 CP (direct gap) that is outside the energy range of our spectrometer. The dominant term is again the Debye-Waller term of the valence band (which causes a shift of 130 meV between 0 and 300 K). If all terms (self-energy, Debye-Waller, and thermal expansion) are included, we obtain an energy difference of about 100 meV between 0 and 300 K, in reasonable agreement with the observed[74] shift of 86 meV. A proper inclusion of the spin-orbit splitting Δ_0 may decrease this disagreement. The calculated linear temperature coefficient of the E_0 gap (in comparison with experimental data) is given in Table IV.

The self-energy term of the electron-phonon interaction causes not only a shift of the electronic states with temperature (due to virtual transitions), but also temperature-dependent lifetime broadenings due to real transitions. A hole in the highest valence band at L for example can scatter to the split-off valence band near Γ by emitting or absorbing a zone-edge phonon (intervalley scattering) and therefore has a finite lifetime τ which leads to a lifetime broadening $\Gamma=\hbar/2\tau$. Similar processes are allowed for electrons in the lowest conduction band, but are less probable as the density of energy-conserving final states in the conduction band is much smaller. These broadenings can be calculated in the present framework of the electron-phonon interaction by taking into account the imaginary part of the self-energy term (the real part causes the shifts), as discussed in Ref. 36. The intervalley phonon spectral functions have been calculated for the points $\pi/2a(1,1,1)$ and $\pi/a(1,1,1)$ that are representative of the E_1 transition and for the point $\pi/2a(3,1,1)$ that is in the region of the E_2 transition, with results similar to those shown in Figs. 6 and 7 of Ref. 38. These spectral functions were then integrated over all the phonon occupation states and the contributions of the valence and conduction band were added up to give the temperature dependence of the CP's. The results are shown by the dotted (E_1 CP) and dashed lines (E_2 CP) in Fig. 7. Details of these broadenings will be discussed elsewhere.

V. CONCLUSION

A detailed study of interband critical points in GaSb has been performed by analyzing the temperature-dependent real and imaginary parts of the dielectric function, as obtained by spectroscopic rotating-analyzer ellipsometry. The critical-point parameters as a function of temperature, especially the energies and broadenings, have been obtained by a full line-shape analysis. The rigid pseudo-ion model (which was used previously to study intervalley scattering processes in GaP and GaAs and shifts and broadenings for Ge, Si, and GaAs) has been found to give a reasonably good description of the observed temperature shifts and lifetime broadenings in GaSb.

ACKNOWLEDGMENTS

We would like to thank S. Logothetidis and J. Kircher for stimulating discussions and a critical reading of the manuscript; H. Hirt, M. Siemers, and P. Wurster for expert technical help; and A. Böhringer for the sample preparation.

*Present address: Centro Nacional de Microelectrónica, Consejo Superior de Investigaciones Científicas, Serrano 144, E-28006 Madrid, Spain.

†Permanent address: Department of Solid State Physics, Faculty of Science, Masaryk University, Kotlářská 2, 611 37 Brno, Czechoslovakia.

‡To whom all correspondence should be addressed.

[1]H. Schweizer, E. Zielinski, S. Hausser, R. Stuber, M. H. Pilkuhn, G. Griffiths, H. Kroemer, and S. Subbanna, IEEE J. Quantum Electron. **QE-23**, 977 (1987).

[2]A. E. Drakin, P. G. Eliseev, B. N. Sverdlov, A. E. Bochkarev, L. M. Dolginov, and L. V. Druzhinina, IEEE J. Quantum Electron. **QE-23**, 1089 (1987).

[3]M. Takeshima, J. Appl. Phys. **56**, 2502 (1984).

[4]A. F. J. Levi and T. H. Chiu, Solid-State Electron. **31**, 625 (1988).

[5]E. E. Mendez, C. A. Chang, H. Takaoka, L. L. Chang, and L. Esaki, J. Vac. Sci. Technol. B **1**, 152 (1983).

[6]G. Griffiths, K. Mohammed, S. Subbanna, H. Kroemer, and J. L. Merz, Appl. Phys. Lett. **43**, 1059 (1983).

[7]H.-J. Gossmann, B. A. Davidson, G. J. Gualtieri, G. P. Schwartz, A. T. Macrander, S. E. Slusky, M. H. Grabow, and W. A. Snyder, J. Appl. Phys. **66**, 1687 (1989).

[8]D. L. Mathine, S. M. Durbin, R. L. Gunshor, M. Kobayashi, D. R. Menke, Z. Pei, J. Gonsalves, N. Otsuka, Q. Fu, M. Hagerott, and A. V. Nurmikko, Appl. Phys. Lett. **55**, 268 (1989).

[9]P. V. Santos, A. K. Sood, M. Cardona, K. Ploog, Y. Ohmori, and H. Okamoto, Phys. Rev. B **37**, 6381 (1988).

[10]U. Cebulla, S. Zollner, A. Forchel, S. Subbanna, G. Griffiths, and H. Kroemer, Solid-State Electron. **31**, 507 (1988).

[11]C. Alibert, A. Joullié, A. M. Joullié, and C. Ance, Phys. Rev. B **27**, 4946 (1983).

[12]J. C. DeWinter, M. A. Pollack, A. K. Srivastava, and J. L. Zyskind, J. Electron. Mater. **14**, 729 (1985).

[13]L. Van Hove, Phys. Rev. **89**, 1189 (1953).

[14]M. Cardona, *Modulation Spectroscopy* (Academic, New York, 1969).

[15]D. E. Aspnes, in *Handbook on Semiconductors,* edited by M. Balkanski (North-Holland, Amsterdam, 1980), Vol. 2, Chap. 4A.

[16]L. Viña, S. Logothetidis, and M. Cardona, Phys. Rev. B **30**, 1979 (1984).

[17]S. Logothetidis, L. Viña, and M. Cardona, Phys. Rev. B **31**, 947 (1985).

[18]L. Viña, H. Höchst, and M. Cardona, Phys. Rev. B **31**, 958 (1985).

[19]S. Logothetidis, P. Lautenschlager, and M. Cardona, Phys. Rev. B **33**, 1110 (1986).

[20]S. Logothetidis, M. Cardona, P. Lautenschlager, and M. Garriga, Phys. Rev. B **34**, 2458 (1986).

[21]P. Lautenschlager, M. Garriga, S. Logothetidis, and M. Car-

dona, Phys. Rev. B **35**, 9174 (1987).
[22]P. Lautenschlager, M. Garriga, and M. Cardona, Phys. Rev. B **36**, 4813 (1987).
[23]S. Zollner, J. Kircher, M. Cardona, and S. Gopalan, Solid-State Electron. **32**, 1585 (1989).
[24]L. Viña and M. Cardona, Phys. Rev. B **29**, 6739 (1984).
[25]L. Viña and M. Cardona, Phys. Rev. B **34**, 2586 (1986).
[26]L. Viña, C. Umbach, M. Cardona, and L. Vodopyanov, Phys. Rev. B **29**, 6752 (1984).
[27]P. Lautenschlager, S. Logothetidis, L. Viña, and M. Cardona, Phys. Rev. B **32**, 3811 (1985).
[28]S. Logothetidis, M. Alouani, M. Garriga, and M. Cardona, Phys. Rev. B **41**, 2959 (1990).
[29]D. E. Aspnes and A. A. Studna, Phys. Rev. B **27**, 985 (1983).
[30]E. Antončik, Czech. J. Phys. **5**, 449 (1955).
[31]J. Camassel and D. Auvergne, Phys. Rev. B **12**, 3258 (1975).
[32]H. Y. Fan, Phys. Rev. **82**, 900 (1951).
[33]P. B. Allen and M. Cardona, Phys. Rev. B **23**, 1495 (1981); **24**, 7479(E) (1981).
[34]P. B. Allen and M. Cardona, Phys. Rev. B **27**, 4760 (1983).
[35]P. Lautenschlager, P. B. Allen, and M. Cardona, Phys. Rev. B **31**, 2163 (1985).
[36]P. Lautenschlager, P. B. Allen, and M. Cardona, Phys. Rev. B **33**, 5501 (1986).
[37]C. K. Kim, P. Lautenschlager, and M. Cardona, Solid State Commun. **59**, 797 (1986).
[38]S. Gopalan, P. Lautenschlager, and M. Cardona, Phys. Rev. B **35**, 5577 (1987).
[39]S. Zollner, S. Gopalan, M. Garriga, J. Humlíček, and M. Cardona, in *Nineteenth International Conference on the Physics of Semiconductors, Warsaw, 1988,* edited by W. Zawadzki (Institute of Physics, Polish Academy of Sciences, Warsaw, 1988), p. 1513.
[40]M. L. Cohen and J. R. Chelikowsky, *Electronic Structure and Optical Properties of Semiconductors* (Springer, Berlin, 1988), pp. 118ff.
[41]C. Benoit à la Guillaume and P. Lavallard, J. Phys. Chem. Solids **31**, 411 (1970).
[42]W. Rühle, W. Jakowetz, C. Wölk, R. Linnebach, and M. Pilkuhn, Phys. Status Solidi B **73**, 255 (1976).
[43]G. Benz and R. Conradt, in *Proceedings of the Twelfth International Conference on the Physics of Semiconductors, Stuttgart, 1974,* edited by M. Pilkuhn (Teubner, Stuttgart, 1974), p. 1262.
[44]G. Benz and R. Conradt, Phys. Rev. B **16**, 843 (1977).
[45]S. C. Chen and Y. K Su, J. Appl. Phys. **66**, 350 (1989).
[46]V. Roberts and J. E. Quarrington, J. Electron. **1**, 152 (1955-56).
[47]W. M. Becker, A. K. Ramdas, and H. Y. Fan, J. Appl. Phys. Suppl. **32**, 2094 (1961).
[48]E. J. Johnson and H. Y. Fan, Phys. Rev. **139**, A1991 (1965).
[49]M. Cardona and G. Harbeke, J. Appl. Phys. **34**, 813 (1963).
[50]S. Zwerdling, B. Lax, K. J. Button, and L. M. Roth, J. Phys. Chem. Solids **9**, 320 (1959).
[51]W. Dreybrodt, W. Richter, F. Cerdeira, and M. Cardona, Phys. Status Solidi B **60**, 145 (1973).
[52]K. Aoki, A. K. Sood, H. Presting, and M. Cardona, Solid State Commun. **50**, 287 (1984).
[53]H. Mathieu, J. Phys. (Paris) **29**, 522 (1968).
[54]M. L. Cohen and J. C. Phillips, Phys. Rev. **139**, A912 (1965); G. W. Gobeli and F. G. Allen, *ibid.* **127**, 141 (1962).
[55]T. C. Chiang and D. E. Eastman, Phys. Rev. B **22**, 2940 (1980).
[56]A. Filion and E. Fortin, Phys. Rev. B **8**, 3852 (1973).
[57]J. Tauc and A. Abrahàm, *Proceedings of the International Conference on Semiconductor Physics, Prague, 1960* (Publishing House of the Czechoslovak Academy of Sciences, Prague, 1961), p. 375.
[58]F. Lukeš and E. Schmidt, *Proceedings of the International Conference on Semiconductor Physics, Exeter, 1962* (Institute of Physics, London, 1963), p. 389.
[59]M. Cardona, J. Appl. Phys. **32**, 2151 (1961); Z. Phys. **161**, 99 (1961).
[60]D. L. Greenaway, Phys. Rev. Lett. **9**, 97 (1962).
[61]M. Cardona, in *Physics of Semiconductors,* Proceedings of the Seventh International Conference, Paris, 1964, edited by M. Hulin (Dunod, Paris, 1964), p. 181.
[62]S. S. Vishnubhatla and J. C. Woolley, Can. J. Phys. **46**, 1769 (1968).
[63]M. Cardona, Phys. Rev. B **15**, 5999 (1977).
[64]E. Matagui, A. G. Thompson, and M. Cardona, Phys. Rev. **176**, 950 (1968).
[65]M. Caronda, K. L. Shaklee, and F. H. Pollak, Phys. Rev. **154**, 696 (1967).
[66]B. J. Parsons and H. Piller, Solid State Commun. **9**, 767 (1971).
[67]D. E. Aspnes, C. G. Olson, and D. W. Lynch, Phys. Rev. B **14**, 4450 (1976).
[68]R. R. L. Zucca and Y. R. Shen, Phys. Rev. B **1**, 2668 (1970).
[69]T. Tuomi, M. Cardona, and F. H. Pollak, Phys. Status Solidi **40**, 227 (1970).
[70]M. Welkowsky and R. Braunstein, Phys. Rev. B **5**, 497 (1972).
[71]M. Reine, R. L. Aggarwal, and B. Lax, Solid State Commun. **8**, 35 (1970).
[72]R. L. Aggarwal, in *Semiconductors and Semimetals,* edited by R. K. Willardson and A. C. Beer (Academic, New York, 1972), Vol. 9, p. 151.
[73]S. O. Sari, Solid State Commun. **12**, 705 (1973).
[74]*Numerical Data and Functional Relationships in Science and Technology,* edited by O. Madelung (Springer, Berlin, 1987), Vol. 22a.
[75]R. J. Elliot, Phys. Rev. **108**, 1384 (1957).
[76]M. Cardona, in *Atomic Structure and Properties of Solids,* edited by E. Burstein (Academic, New York, 1972), p. 541.
[77]A. R. Goñi, K. Strössner, K. Syassen, and M. Cardona, Phys. Rev. B **36**, 1581 (1987).
[78]S. Zollner, C. Lin, E. Schönherr, A. Böhringer, and M. Cardona, J. Appl. Phys. **66**, 383 (1989).
[79]D. E. Aspnes, B. Schwartz, A. A. Studna, L. Derick, and L. A. Koszi, J. Appl. Phys. **48**, 3510 (1977).
[80]D. E. Apsnes and A. A. Studna, Rev. Sci. Instrum. **49**, 291 (1978).
[81]A. Savitzky and M. J. E. Golay, Anal. Chem. **36**, 1627 (1964); corrections in J. Steinier, Y. Termonia, and J. Deltour, *ibid.* **44**, 1906 (1972).
[82]J. W. Garland, C. Kim, H. Abad, and P. M. Raccah, Phys. Rev. B **41**, 7602 (1990).
[83]M. Alouani, L. Brey, and N. E. Christensen, Phys. Rev. B **37**, 1167 (1988).
[84]C. J. Bradley and B. L. Davies, J. Math. Phys. (N.Y.) **11**, 1536 (1970).
[85]D. E. Aspnes and A. A. Studna, Phys. Rev. B **7**, 4605 (1973).
[86]R. M. Wentzcovitch, M. Cardona, M. L. Cohen, and N. E. Christensen, Solid State Commun. **67**, 927 (1988).
[87]J. R. Chelikowsky and M. L. Cohen, Phys. Rev. B **14**, 556 (1976).
[88]G. G. Wepfer, T. C. Collins, and R. N. Euwema, Phys. Rev. B **4**, 1296 (1971).

[89]F. Herman, R. L. Kortum, C. D. Kuglin, and J. P. Van Dyke, *Methods in Computational Physics,* edited by B. Adler, S. Fernbach, and M. Rotenberg (Academic, New York, 1968), Vol. 8, p. 163.
[90]M. Cardona, N. E. Christensen, and G. Fasol, Phys. Rev. B **38**, 1806 (1988).
[91]R. Braunstein and E. O. Kane, J. Phys. Chem. Solids **23**, 1423 (1962).
[92]K. C. Rustagi, P. Merle, D. Auvergne, and H. Mathieu, Solid State Commun. **18**, 1201 (1976).
[93]J. A. Van Vechten, Phys. Rev. **187**, 1007 (1969).
[94]Z.-Q. Gu, M.-F. Li, J.-Q. Wang, and B.-S. Wang, Phys. Rev. B **41**, 8333 (1990).
[95]Y. P. Varshni, Physica (Utrecht) **34**, 149 (1967).
[96]A. Manoogian and J. C. Woolley, Can. J. Phys. **62**, 285 (1984).
[97]*Numerical Data and Functional Relationships in Science and Technology,* edited by K. H. Hellwege (Springer, Berlin, 1982), Vol. 17a.
[98]S. I. Novikova, in *Semiconductors and Semimetals,* edited by R. K. Willardson and A. C. Beer (Academic, New York, 1966), Vol. 2, p. 33.
[99]Don L. Camphausen, G. A. Neville Connell, and W. Paul, Phys. Rev. Lett. **26**, 184 (1971).
[100]P. B. Allen and V. Heine, J. Phys. C **9**, 2305 (1976).
[101]J. S. Reid, Acta Crystallogr. Sect. A **39**, 1 (1983).
[102]J. F. Vetelino, S. P. Gaur, and S. S. Mitra, Phys. Rev. B **5**, 2360 (1972).
[103]M. L. Cohen and T. K. Bergstresser, Phys. Rev. **141**, 789 (1966).
[104]K. Kunc and H. Bilz, Solid State Commun. **19**, 1027 (1976).
[105]K. Kunc and O. H. Nielsen, Comput. Phys. Commun. **16**, 181 (1979); **17**, 413 (1979).
[106]S. Zollner, S. Gopalan, and M. Cardona, in *Phonons 89,* Proceedings of the Third International Conference on Phonon Physics and Sixth International Conference on Phonon Scattering in Condensed Matter, edited by S. Hunklinger, W. Ludwig, and G. Weiss (World Scientific, Singapore, 1990), Vol. 2, p. 787.
[107]D. Strauch and B. Dorner, J. Phys. C **19**, 2853 (1986).
[108]M. K. Farr, J. G. Traylor, and S. K. Sinha, Phys. Rev. B **11**, 1587 (1975); corrections in Ref. 101.